

## Intrinsic surface states of (110) surfaces of group IV and III-V semiconductors\*

J. D. Joannopoulos<sup>†</sup> and Marvin L. Cohen

*Department of Physics, University of California, Berkeley, California 94720*

*and Inorganic Materials Research Division, Lawrence Berkeley Laboratory, Berkeley, California 94720*

(Received 25 July 1974)

Electronic local and total density of states calculations have been performed using tight binding models on the (110) surface of a group IV and III-V semiconductor. Ge and GaAs are taken as prototypes and the surface is assumed to be unrelaxed. Several new surface states are obtained near the bottom of the valence bands. The origin, localization, and character of the surface states are examined.

### I. INTRODUCTION

Recently tight-binding models with only  $sp^3$  hybrids<sup>1,2</sup> (or  $s$  and  $p$  orbitals<sup>3</sup>) and with all nearest-neighbor interactions included have been found very useful in studying the (111) surfaces of group IV<sup>1,2</sup> and III-V<sup>3</sup> semiconductors. This usefulness results not only from the simplicity and calculational convenience of the methods but also because these models are very appealing from a physical point of view. They can reproduce results obtained from experiment<sup>4</sup> and from more elaborate theoretical methods.<sup>5</sup>

We wish to extend some of these models to study the (110) surfaces of semiconductors. This surface is of interest since it is the thermally stable cleavage face of III-V compounds and remains unreconstructed. Moreover, it is of intrinsic interest since two different types of atoms can exist simultaneously on the surface, so that the surface states can exhibit the individual characteristics of each atom.

Using this method we recently briefly reported<sup>6</sup> the existence of new states for *unrelaxed* (110) surfaces of Ge and GaAs. In this paper we develop the method in detail and examine the origin, localization, and character of the surface states. We also present local density-of-states calculations for atoms in various surface layers. The results presented here are generally of wider validity than just for the cases of Ge and GaAs; i.e., Ge and GaAs will be considered as prototypes.

The format of the paper is as follows. In Sec. II we discuss the tight-binding model, describe the structural aspects of the system we are studying, and discuss the calculational methods involved. In Sec. III we present the results of our calculations for Ge and GaAs and discuss their ramifications. Finally, in Sec. IV we make some concluding remarks.

The model we use to study the (110) surface of a diamond structure or zinc-blende semiconductor is similar to a model used first by Hirabayashi<sup>1</sup>

for (111) and (100) surfaces. The method involves studying a system of atoms which is finite in one dimension and periodic in the other two dimensions. We are thus dealing with a "slab" of material with two surface layers which can be chosen to have  $N$  periodic layers of atoms. It is found<sup>1</sup> that generally reliable results can be obtained with  $N \geq 10$ , so that one need not worry about spurious results caused by the finiteness and double-surface characteristics of the system.

This system will now be conveniently and "realistically" studied using a tight-binding model with  $sp^3$  (or  $s$  and  $p$ ) orbitals, including all interactions between nearest-neighbor atoms. These interactions can be parametrized and fitted to realistic (e.g., pseudopotential) band structures with very good precision. In general, the filled valence bands are obtained much more accurately than the conduction bands. This is reasonable because of the plane-wave-like nature of conduction bands. This should have relevant consequences only for the detailed structure of the surface states in the fundamental gap.

### II. CALCULATIONAL PROCEDURES

In Fig. 1 we show a sketch of (110) layers of atoms lying parallel to the  $\hat{x}$ - $\hat{y}$  plane. Two different types of atoms are shown as they would occur in a zinc-blende structure. We also show schematically four  $sp^3$ -like directed orbitals on each of the two atoms in a surface unit cell ( $ABCD$ ). For a zinc-blende structure the (110) surface thus contains one dangling orbital from the cation and one from the anion per unit cell. In the case of a diamond-structure (110) surface the two atoms and dangling orbitals are identical, but there are still two atoms in a surface unit cell.

In the tight-binding model we are considering, we saturate the number of nearest-neighbor interactions. Using the orbital notation (to be discussed shortly) shown at the bottom of Fig. 1, we must specify the following interaction parameters for a homopolar system:

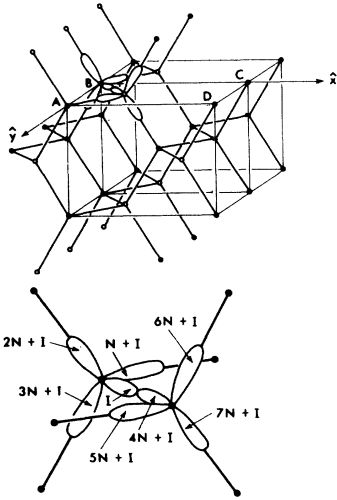


FIG. 1. Drawing (top) of (110) layers of atoms shown parallel to the  $\hat{x}\hat{y}$  axis for a zinc-blende structure. The dots and open circles represent atoms and the heavy lines signify bonds.  $ABCD$  defines the surface unit cell and four  $sp^3$ -like directed orbitals are sketched on each of the two basis atoms. Below we show the notation used in the text to label the orbitals for any given layer  $I$  in a total system of  $N$  layers.

$$\begin{aligned}
 V_0 &= \langle I | H | I \rangle, \\
 V_1 &= \langle I | H | N+I \rangle, \\
 V_2 &= \langle I | H | 4N+I \rangle, \\
 V_3 &= \langle I | H | 5N+I \rangle, \\
 V_4 &= \langle N+I | H | 6N+I \rangle, \\
 V_5 &= \langle N+I | H | 5N+I \rangle.
 \end{aligned} \tag{1}$$

For all practical purposes  $V_0$  can be taken as zero, since it simply involves a reference energy for all the bands. For Ge these parameters were fit to pseudopotential band structures<sup>7</sup> and the agreement is fairly good. The values obtained (in eV) are  $V_0=0$ ,  $V_1=-2.0$ ,  $V_2=-5.0$ ,  $V_3=-0.2$ ,  $V_4=-0.4$ , and  $V_5=0.6$ .

For GaAs we would, in principle, need to break down some of the parameters in (1) into additional parameters because of the lack of inversion symmetry. It is, however, quite simple, convenient, and adequate, for our purposes, to describe GaAs with only one additional parameter. Namely, we take  $V_0 = \pm \Delta$  depending on whether  $|I\rangle$  in (1) is a cation ( $+\Delta$ ) or anion ( $-\Delta$ ) orbital. With  $\Delta = 3.2$  eV we obtain an "antisymmetric" gap in the filled valence band which is in satisfactory agreement with pseudopotential calculations.<sup>7</sup> As we have already mentioned, our results are generally valid, so that Ge and GaAs can be considered as prototypes. Therefore it is unnecessary to obtain fits which are in *excellent* agreement with experiments.

In the structural model the most important parameter to specify is the number  $N$  of layers of atoms. Once this is done the labels of each orbital in the unit cell for any layer  $I$  can be very conveniently specified, as shown at the bottom of Fig. 1. In addition, the tight-binding Hamiltonian matrix can be obtained easily and involves essentially only two matrices for any layer  $I$ . Given the unit cell ( $ABCD$ ) and the  $\hat{x}\hat{y}$  coordinate system as shown in Fig. 1 we obtain the following Hamiltonian submatrices for any layer  $I$ :

	$I$	$N+I$	$2N+I$	$3N+I$	$4N+I$	$5N+I$	$6N+I$	$7N+I$
$I$	$-\Delta$	$V_1$	$V_1$	$V_1$	$V_2 + V_5\eta^*$	$V_3 + V_3\eta^*$	$V_3 + V_4\eta^*$	$V_3 + V_4\eta^*$
$N+I$		$-\Delta$	$V_1$	$V_1$	$V_3 + V_3\eta^*$	$V_5 + V_2\eta^*$	$V_4 + V_3\eta^*$	$V_4 + V_3\eta^*$
$2N+I$			$-\Delta$	$V_1$	$V_3 + V_4\eta^*$	$V_4 + V_3\eta^*$	$V_4 + V_4\eta^*$	$V_5 + V_5\eta^*$
$3N+I$				$-\Delta$	$V_3 + V_4\eta^*$	$V_4 + V_3\eta^*$	$V_5 + V_5\eta^*$	$V_4 + V_4\eta^*$
$4N+I$					$\Delta$	$V_1$	$V_1$	$V_1$
$5N+I$						$\Delta$	$V_1$	$V_1$
$6N+I$							$\Delta$	$V_1$
$7N+I$								$\Delta$

and

$$\begin{array}{cccccccc}
4N+I-1 & 5N+I-1 & 6N+I-1 & 7N+I-1 & 4N+I+1 & 5N+I+1 & 6N+I+1 & 7N+I+1 \\
I & H_5^I & H_4^I & H_4^I & H_3^I & H_5^I & H_4^I & H_3^I & H_4^I \\
N+I & H_4^I & H_5^I & H_4^I & H_3^I & H_4^I & H_5^I & H_3^I & H_4^I \\
2N+I & H_3^I & H_3^I & H_3^I & H_2^I & H_4^I & H_4^I & H_3^I & H_5^I \\
3N+I & H_4^I & H_4^I & H_5^I & H_3^I & H_3^I & H_3^I & H_2^I & H_3^I
\end{array}, \quad (3)$$

where

$$\eta = e^{ik_y a / \sqrt{2}}, \quad \xi = e^{ik_x a}, \quad (4)$$

and

$$H_n^I = \frac{1}{2} V_n (1 + \eta^* \xi^*) - \frac{1}{2} V_n (-1)^I (1 - \eta^* \xi^*). \quad (5)$$

Here  $a$  is the lattice constant and expression (5) is different depending on whether  $I$  is an even- or odd-numbered layer. We define all odd-numbered layers to be analogous to the  $ABCD$  layer shown in Fig. 1, where there is always one basis atom at the origin. The information contained in (2) and (3) is all that is necessary to build up the complete Hermitian Hamiltonian matrix for any given number of layers  $N$ . However, care must be taken if  $I$  is a surface layer (i.e.,  $I=1$  or  $I=N$ ). In this case some of the elements in submatrix (3) must be treated differently, depending on what type of relaxation is imposed. In our calculations we assumed an unrelaxed surface and just set the appropriate matrix elements to zero. The other matrix elements associated with the surface layer itself and its interaction with the second layer are taken to be the same as in the bulk. We have thus neglected the effects of charge transfer and changes in Madelung energy. In principle, these along with relaxation effects should be included. In the present calculation, however, our aim is primarily concerned with showing the existence of certain surface states. We expect that the main effect of including matrix-element differences would be to cause changes in the positions of these states and some changes in amplitude. For example, to first order, the  $B_3$  states in Fig. 2 would be expected to move further into the heteropolar gap. This would be caused by a decrease in the effective Madelung potential acting on the anion surface atoms.

Once the band structure is known the total density of states can be obtained using the expression

$$N(E) = \frac{1}{MN_a} \sum_{\vec{k}} \sum_n \delta(E - E_n(\vec{k})), \quad (6)$$

where  $N_a$  is the number of atoms in the primitive cell,  $M$  is the number of primitive cells, and  $N(E)$  is normalized to the number of states per atom. The local density of states of an orbital is defined

as

$$N_{ij}(E) = \frac{1}{MN_a} \sum_{\vec{k}} \sum_n |\langle \psi_{\vec{k},n}^* | \phi_{\vec{k},ij} \rangle|^2 \delta(E - E_n(\vec{k})), \quad (7)$$

where  $\psi_{\vec{k},n}$  is an eigenfunction of the total Hamiltonian and  $\phi_{\vec{k},ij}$  is the  $j$ th Bloch-function orbital centered at atom  $i$ . The local density of states of an atom is then obtained from

$$N_i(E) = \sum_j N_{ij}(E). \quad (8)$$

Physically the local density of states  $N_i(E)$  is just equal to a product of the total density of states  $N(E)$  multiplied by an average probability that an electron is at atom  $i$  when the electron has an energy  $E$  in the total system.

The method used to evaluate the integrals in (6) and (7) is due to Gilat and Raubenheimer.<sup>9</sup> The energy derivatives required by this method were obtained using  $\vec{k} \cdot \vec{p}$  perturbation theory. In Sec. III we show the results of our calculations for a system with 12 layers of atoms. The local densities of states that will be shown will involve an additional factor of  $2N$  in order to make the normaliza-

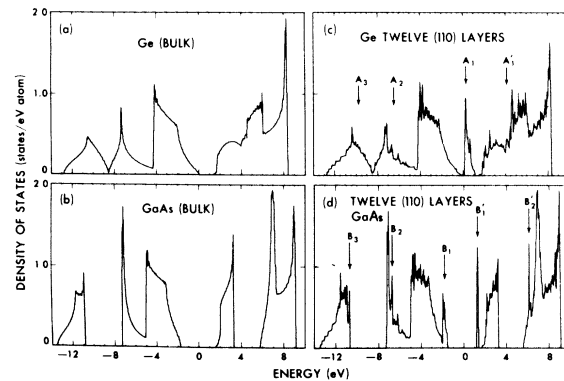


FIG. 2. Total densities of states for Ge and GaAs in the diamond and zinc-blende structures [(a) and (b)] and in structures consisting of 12 layers of atoms with unrelaxed (110) surfaces [(c) and (d)], respectively. These densities of states are obtained using the tight-binding model discussed in the text. The labels A and B represent surface states for Ge and GaAs, respectively, and are also described in the text.

tion the same as for the total density of states and hence make comparisons easier.

### III. RESULTS

In Figs. 2(a) and 2(b) we show the total density of states of Ge and GaAs in the diamond and zinc-blende structures, respectively. The filled valence bands are shown at negative energies. The shapes of these curves are in very good over-all agreement with the densities of states obtained from pseudopotential calculations.<sup>7</sup> The biggest discrepancy in the valence band results from an inability to reproduce the dip in the  $p$ -like states between  $\Sigma_1^{\text{min}}$  and  $X_4$ , which would lie near  $-4$  eV. This is, however, unimportant and can actually be obtained by introducing a second-nearest-neighbor interaction.<sup>9</sup>

In Figs. 2(c) and 2(d) we show the total density of states for Ge and GaAs in the 12-layer structure, respectively. The Fermi levels for Ge and GaAs are around 0.4 and 0 eV, respectively. These are unsmoothed computer plots, so that the wiggles along the curves should be considered as noise. The steplike structure around  $-12$  eV is, however, real and is caused by the two-dimensional singularities of a finite number of two-dimensional layers. Figures 2(c) and 2(d) reveal a composite effect of bulk and surface properties. They can, for instance, be compared readily with their completely bulk counterparts shown in Figs. 2(a) and 2(b). The labels A and B represent surface states obtained for Ge and GaAs in these calculations. We now proceed to analyze them in detail.

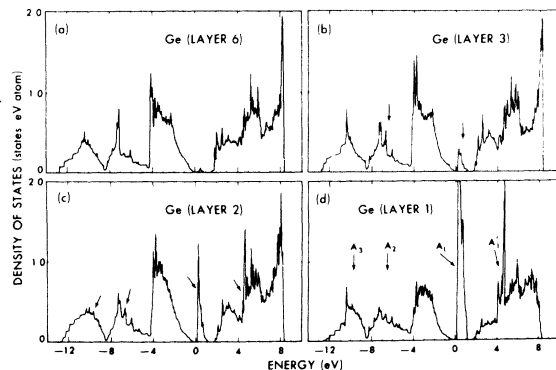


FIG. 3. Local densities of states for a Ge atom in the sixth (a), third (b), second (c), and outer-surface (d) layers of the 12-layer structure. The arrows in the figures represent the onset of surface states as the surface layer 1 is approached from within the bulk. The labels  $A_1$ ,  $A_2$ ,  $A_3$ , and  $A_1'$  refer to surface states discussed in the text.

### A. Ge

In Fig. 3 we show a plot of the local densities of states of a Ge atom in various layers of atoms in the 12-layer system. The second basis atom in each layer is identical to the first, so that their local densities of states are equivalent. In Fig. 3(a) we show the local density of states for a Ge atom in the sixth layer from the surface. This then is essentially a bulk density of states, as is readily observed by comparing Fig. 3(a) with Fig. 2(a). Let us now examine what happens as we approach the surface. Nothing really happens until we get to the third layer of atoms shown in Fig. 3(b). We can now distinguish clearly the onset of two types of surface states shown by arrows in the figure. When we go to the second layer the former states become more pronounced and we have the onset of two other additional surface states, also designated by arrows in this figure. Finally, when we reach the outer surface layer [Fig. 3(d)], the states in the fundamental gap become very strong and go off the scale. Actually, the number of states in the fundamental gap of Fig. 3(d) is around 1.5 states/atom. These states are labeled  $A_1$  and are the usual states obtained in the gap from other calculations. They consist of two surface bands and represent the dangling bond states of Ge atoms at the surface. In our calculations we find that approximately 85% of the charge is concentrated in the first layer, with 98% of this charge in the first three surface layers. This is, of course, consistent with the trends shown in Fig. 3. The states labeled  $A_2$  designate new surface states<sup>6</sup> which originate near  $\bar{M}$  and along  $\bar{M}$  to  $\bar{X}'$  and are concentrated primarily in the first three layers. This concentration is also observed by comparing Figs. 3(a)–3(d). These states represent bond states that lie in the layers with roughly 30% of the charge localized in each layer. The states labeled  $A_3$  are also new<sup>6</sup> and occur mostly at and near  $\bar{X}'$ , but extend along  $\bar{X}'$  to  $\bar{\Gamma}$  and  $\bar{X}'$  to  $\bar{M}$  with a total bandwidth of around 1 eV. These states represent essentially Ge  $s$ -like states with about 64% of the charge concentrated in the first layer, with additional concentrations in either the second ( $\bar{X}'$  to  $\bar{\Gamma}$ ) or third ( $\bar{X}'$  to  $\bar{M}$ ) layers.

Finally, let us also briefly discuss for completeness the  $A_1'$  surface states obtained in the conduction band. These originate from two areas in the irreducible zone. The states at 4.4–4.6 eV originate from a region near the center of the irreducible zone. They are mostly concentrated in the first two atomic layers and are essentially antibonding  $s$ -like states in nature. The states between 4.0 and 4.4 eV originate mainly around  $\bar{X}'$  and contain roughly 80% of the charge in the first layer.

They are localized on hybrid orbitals lying along the surface. The concentrations of the  $A'_1$  states are also rescaled in the local density-of-states plots in Fig. 3.

### B. GaAs

In Figs. 4 and 5 we show plots of the local densities of states of an As and a Ga atom, respectively, in various layers of atoms in the 12-layer structure. Again, as in Ge, we concentrate on the sixth, third, and second, and outer layers of atoms. Since the local densities of states of layer 6 can essentially be interpreted as a bulk local density of states, Figs. 4(a) and 5(a) reveal the As and Ga character of the various regions of the bulk or crystalline [Fig. 2(b)] density of states. We notice that the filled valence band is mostly of As nature. This is particularly true in the  $s$ -like region of the density of states (around  $-12$  eV). The region around  $-6$  eV is essentially equally shared between As and Ga states, while the top of the valence band is again predominantly As-like. In the tight-binding model the lower-energy conduction-band states are also equally Ga- and As-like, while the higher-energy conduction-band states are strongly Ga in nature.

Let us now examine what happens as we approach the surface. In Figs. 4(b) and 5(b) we show the local density of states of an As and a Ga atom, respectively, in the third layer. We can distinguish clearly the onset of four types of surface states shown by arrows in the figures. The states near  $-11$  and  $-2$  eV are very strongly As in nature, while the states near  $1$  eV are predominantly Ga in character. Finally, the surface states near  $-7$

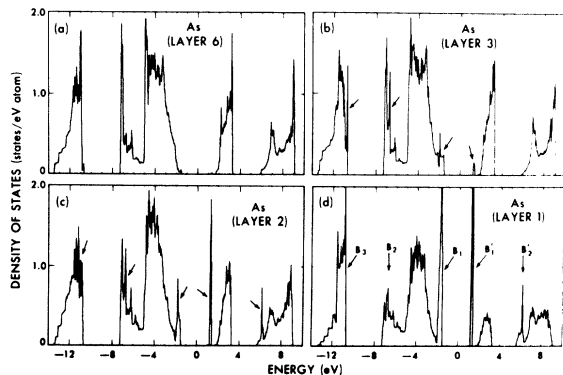


FIG. 4. Local densities of states for an As atom in the sixth (a), third (b), second (c), and outer-surface (d) layers of the 12-layer structure. The arrows in the figures represent the onset of surface states as the surface layer 1 is approached from within the bulk. The labels  $B_1$ ,  $B_2$ ,  $B_3$ ,  $B'_1$ , and  $B'_2$  refer to surface states discussed in the text.

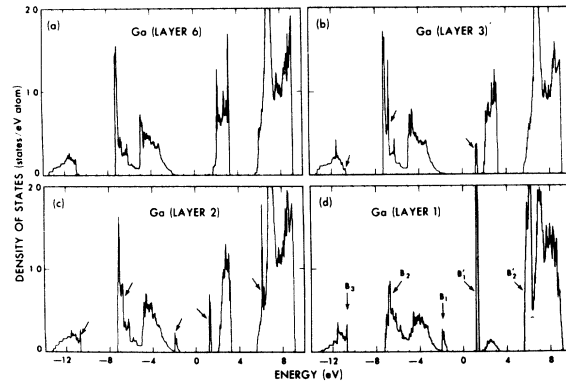


FIG. 5. Local densities of states for a Ga atom in the sixth (a), third (b), second (c), and outer-surface (d) layers of the 12-layer structure. The arrows represent the onset of surface states as the surface layer 1 is approached from within the bulk. The labels  $B_1$ ,  $B_2$ ,  $B_3$ ,  $B'_1$ , and  $B'_2$  refer to surface states discussed in the text.

eV seem to be equally shared between the As and Ga atoms. When we reach the second layer [Figs. 4(c) and 5(c)] we now obtain new surface states in the conduction bands which seem to be of a stronger Ga nature. In addition, the surface state at  $-2$  eV now has some Ga character. Another interesting effect that has occurred is the rapid strengthening of the As character of the surface states near  $1$  eV. In this layer the As nature of these states is stronger than the Ga nature. Finally, when we reach the surface [Figs. 4(d) and 5(d)], all the surface states become more pronounced but there are also some very rapid changes. First, the As character of the  $B_1$  states becomes very strong, while the Ga character does not change very much. There are approximately 1.4 states/atom in the  $B_1$  states of Fig. 4(d). Second, the character of the  $B_1$  states has now become more Ga-like. This is difficult to see from the figures since both peaks have gone off the scales; however, we find about 0.4 states/atom for the  $B'_1$  peak in Fig. 4(d) and about 1.0 states/atom for the  $B'_1$  peak in Fig. 5(d). Finally, the  $B_3$  states in Fig. 4(d) have also become very strong now, with about 1.3 states/atom between  $-11.6$  and  $-10.7$  eV.

The band structures of these surface states are plotted in Fig. 6 along the symmetry lines of the irreducible zone given by  $\bar{\Gamma}X'MX$  in the notation of Jones.<sup>10</sup> The labels on the right-hand side of the figure identify the various bands with the appropriate types of surface states. The dashed lines represent the band edges as obtained from Fig. 2(b) and the first and second numbers in parentheses represent roughly the fraction of charge on the As and Ga atoms, respectively. The  $B_1$  and

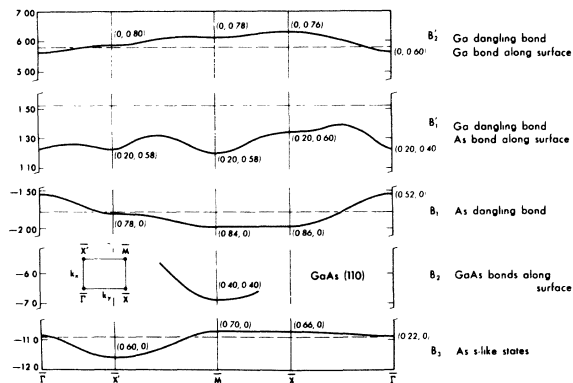


FIG. 6. Surface bands for GaAs along important symmetry directions. The irreducible zone and symmetry points are sketched in the lower left-hand side of the figure. The numbers  $(f_1, f_2)$  represent the fraction of charge  $f_1$  and  $f_2$  concentrated in the first surface layer for an As and Ga atom, respectively, for the various surface states and symmetry points. The labels B refer to surface states discussed in the text and identify their corresponding band structures. The dashed lines represent band edges of the bulk and can be compared with those in Fig. 1(b).

$B_1'$  states are the usual states obtained in the fundamental gap of a polar compound. They essentially result from a splitting of the two  $A_1$  surface bands caused by the differences in potential of the cation and anion. In our calculations we find that the  $B_1$  states represent As dangling bond states with roughly 80% of the charge localized in the first layer. From Fig. 6 we notice that the surface bands cross the bulk edge around  $\bar{\Gamma}$ . However, it is the  $\bar{M}$  and  $\bar{X}$  regions that contain the strongest localization. The  $B_1'$  states are also localized more strongly at  $\bar{M}$  and  $\bar{X}$ . These states contain roughly 80% of the charge in the first layer, with 60% on the Ga atoms and 20% on the As atoms. This is also consistent with the local density-of-states plots in Figs. 4 and 5. The  $B_1''$  states represent dangling bond Ga states along with As bonding states which lie along the surface layer.

The  $B_2$  states are new<sup>6</sup> and originate from a rather small region of the irreducible zone around  $\bar{M}$ . This is shown in Fig. 6, where we also notice that at  $\bar{M}$  we have 80% of the total charge localized in the first layer, which is shared equally between the As and Ga atoms. As we go away from  $\bar{M}$  the charge is primarily concentrated in the first three layers. This is also what was observed in the local densities of states in Figs. 4 and 5. These states represent GaAs bonding states which lie primarily along the surface layer bonds.

The  $B_3$  states are also new<sup>6</sup> and of particular in-

terest since this surface band extends across the bulk edge into the "antisymmetric" or "heteropolar" gap. This is shown quite clearly in Fig. 6, where the band crosses the edge at  $\bar{M}$ ,  $\bar{X}$ , and  $\bar{\Gamma}$ . These states extend approximately 0.2 eV across this edge. The strongest localization occurs at  $\bar{M}$  and  $\bar{X}$  with roughly 70% and 60%, respectively, of the charge localized in the first layer. The  $B_3$  states represent As  $s$ -like states and at  $\bar{\Gamma}$  they are concentrated roughly equally in the first three layers. These states remain extended into the "heteropolar" gap, even with small changes in the tight-binding parameters. In particular, the less ionic the material the more they extend into the gap.

Finally for completeness let us also briefly examine the  $B_2'$  states which are found in our tight-binding conduction bands and also extend across a bulk edge. This is again shown in Fig. 6, where we obtain a crossing in the region around  $\bar{\Gamma}$ . The  $B_2'$  states are a combination of Ga dangling bond states along with charge localized on Ga hybrid orbitals lying along the bonds. The strongest localization is at  $\bar{X}'$  and  $\bar{M}$  with roughly 80% and 78%, respectively, of the charge concentrated in the first layer. The Ga nature and localization of the  $B_2'$  states is also clearly revealed in Figs. 4 and 5.

#### IV. SUMMARY AND CONCLUSIONS

We have studied the (110) surface of a diamond and zinc-blende semiconductor using Ge and GaAs as prototypes. The method used involved a model structure consisting of a finite number of (110) layers of atoms. The surface layers of this structure were assumed to be unrelaxed and the system was studied using a tight-binding model, including all interactions between nearest-neighbor atoms. Taking the structure to contain 12 layers produces reliable results while keeping the computational aspects simple.

Using the tight-binding model whose parameters were fitted adequately to pseudopotential band structures<sup>7</sup> we have calculated local densities of states of atoms for various surface layers. These calculations are very useful and appealing because they reveal in a very natural way how the states behave as one approaches the surface from the bulk. In particular, we have found new surface states which we designate by  $A_2$  and  $A_3$  for Ge and  $B_2$  and  $B_3$  for GaAs. By surface states we mean states which are very well localized on the surface. We make no distinction here between *bona fide* surface states and strong resonances. The  $A_2$ ,  $A_3$ ,  $B_2$ , and  $B_3$  states lie in the lower-energy regions of the filled valence bands where the tight-

binding description is most valid. The surface states  $A_2$  and  $B_2$  are quite similar. They both involve states that originate around  $\bar{M}$  and represent bondlike states which lie along the surface layers. The  $A_3$  and  $B_3$  states are also similar in that they both involve  $s$ -like surface-charge distributions. Of particular interest are the  $B_3$  states, since they extend into the "heteropolar" gap of an ionic compound. This extension should decrease with the increasing ionicity of the material. This diminution of the surface effect with increasing ionicity

is of course related to a general feature of systems which can be described with very localized states. Such systems are affected rather weakly by long-range perturbations.

Finally it should be emphasized that the simplicity and "real-space" nature of the tight-binding model makes it a very useful tool in treating more involved aspects of surface studies. For instance, relaxation and reconstruction effects as well as influences of adsorbates can be studied in rather simple and physical ways.

---

\*Supported in part by the National Science Foundation under Grant No. GH 35688.

†Present address: Department of Physics, MIT, Cambridge, Mass.

<sup>1</sup>K. Hirabayashi, J. Phys. Soc. Jpn. 27, 1475 (1969).

<sup>2</sup>K. C. Pandey and J. C. Phillips, Solid State Commun. 14, 439 (1974).

<sup>3</sup>D. J. Chadi and M. L. Cohen, Phys. Rev. B (to be published).

<sup>4</sup>J. E. Rowe and H. Ibach, Phys. Rev. Lett. 31, 102

(1973).

<sup>5</sup>J. A. Appelbaum and D. R. Hamann, Phys. Rev. Lett. 31, 106 (1973).

<sup>6</sup>J. D. Joannopoulos and M. L. Cohen (unpublished).

<sup>7</sup>J. Chelikowsky, D. J. Chadi, and M. L. Cohen, Phys. Rev. B 8, 2786 (1973).

<sup>8</sup>G. Gilat and L. J. Raubenheimer, Phys. Rev. 144, 390 (1966).

<sup>9</sup>D. J. Chadi and M. L. Cohen (unpublished).

<sup>10</sup>R. O. Jones, Phys. Rev. Lett. 20, 992 (1968).